DAMAGE ANALYSIS OF BRIDGES AFFECTED BY TSUNAMI DUE TO GREAT EAST JAPAN EARTHQUAKE

Kenji Kosa[1]

Abstract

Many bridges were washed away by Tsunami caused by the 2011 Great East Earthquake. We carried out the field survey and investigate the detailed damage to a lot of bridges in Tohoku Region. Utatsu Bridge, a prestressed concrete bridge, suffered enormous damage from the destructive tsunami. The detailed damage and the possible mechanisms of Utatsu Bridge have been conducted. Furthermore, from the study of the relation between β values (ratio between girder resistance and wave lateral load) and bridge damage extents of bridges in Tohoku Region and Sumatra Island, it is noted that ratio β is a significant indicator to judge the damage extent of bridge girders.

Introduction

During the Great East Earthquake, the outflow and excessive scour occurred to more than 300 bridges. **Fig. 1** illustrate the bridges which suffered damage Rank A (bridge is incapable). More than 300 bridges, including 9 national roads, 14 prefectural roads and 101 railroads, suffered serious losses. Despite a lack of official data about the damage to city and village roads, by the use of Google Earth, it is noted that at least 200 bridges suffered serious losses.

Furthermore, the damage extent of the injured parts (girder, substructure, foundation) of bridges in Tohoku region is compared with the damage of bridges in Sumatra Earthquake by authors. **Fig. 2** shows the damage extent to the 26 bridges in the western coast of Sumatra and **Fig. 3** plots the damage extent to the 12 bridges in this tsunami attack. Based on **Fig. 2** and **Fig. 3**, many girders suffered damage Rank A, namely they were washed away entirely due to tsunami action. For substructures, although partial piers flowed out, comparing with girders, the occurrence rate is smaller.

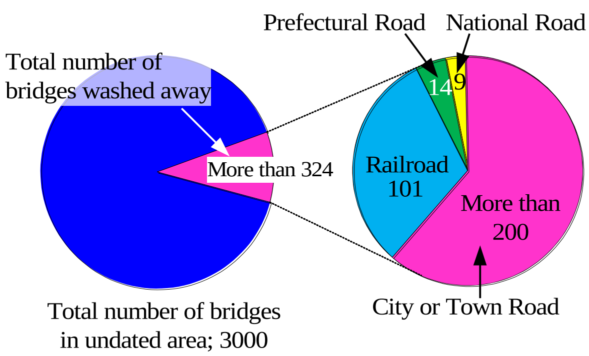

Fig. 1 Amount of bridges washed away

[1] Ph.D, Prof, Dept. of Civil Eng, Kyushu Institute of Technology

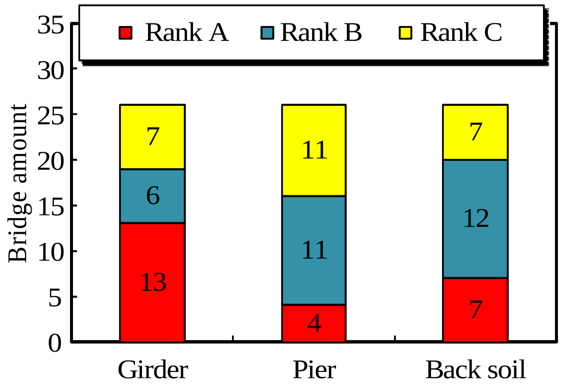

Fig. 2 Damage to bridge due to Sumatra Earthquake

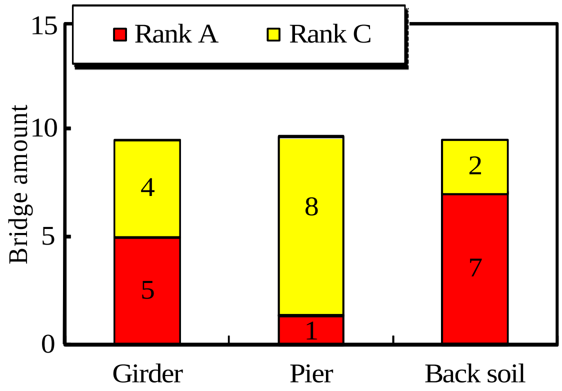

Fig. 3 Damage to bridge due to Great Japan Earthquake

Table 1 Video shot locations

Location		Distancce to Shoreline [m]	Amount of Debris
A	Farm Field in Minamisanriku Town	1200	3
B	Wakabayashiku in Sendai City	1100	3
C	Hachiman River in Minamisanriku Town	1200	6
D	Kamaishi Port in Kamaishi City	0	2
E	Kitakami River in Ishinomaki City	4100	2

Besides that, it is frequent that foundations inflicted damage Rank A. The soils behind abutments were scoured. According to above data, the bridges in the 2 locations, where the wave heights were in excess of 10m, have many common points. The outflow of girders and the scour of foundations are the main damage to bridges.

Wave Height and Velocity

The tsunami arrived 30 minutes after the great earthquake and reached to approximately 5km inland. Further, it is reported the tsunami went upstream about 40km from the mouth of Kitakami River. The wave heights at the extensive region were measured by tidal observation station of Japan Meteorological Agency. For example, the wave height at Miyako was 8.5m, which is the highest one; in addition, the wave height at Oofunato and Souma are higher than 8.0m and 7.3m respectively (Japan Meteorological Agency, 2011). In order to evaluate the wave action on bridges, besides wave height, it is necessary to acquire wave velocities as well. Here, the authors apply the videos shot at the 5 locations in **Table 1**, which are close to shoreline, to estimate the wave velocity (Li, 2011) and these 5 locations are marked by A~E.

The rough measuring process of wave velocity is as follows. In one video, it is able to search for 2 distinguished place points where a pile of floating debris passed through. By using the Google Earth's distance measurer and the timer in video, it is available to obtain the distance between 2 points and the time span for the floating debris flowed from one point to the other. In the end by the Eq. (1), the velocity of

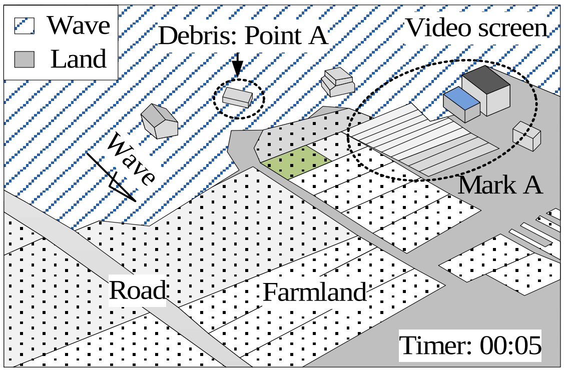

Fig. 4 Starting point for timing

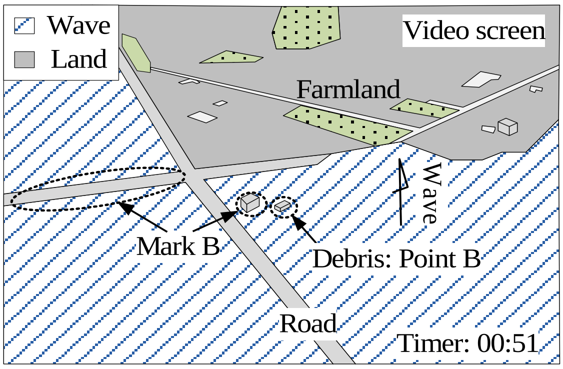

Fig. 5 Terminal point for timing

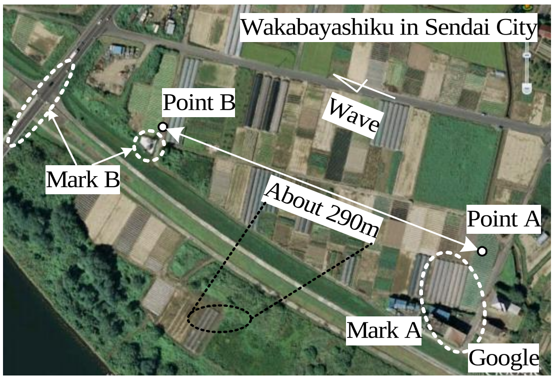

Fig. 6 Distance between 2 points

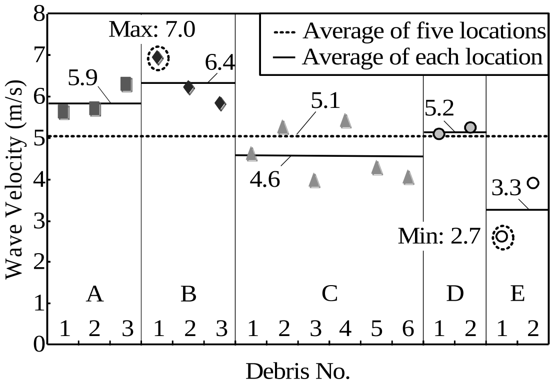

Fig. 7 Velocity result

debris was able to be computed roughly and this velocity can be regarded as the wave velocity at the video shot location.

$$v = \frac{l}{t} \tag{1}$$

Where v is the wave velocity (m/s); l is the distance between 2 place points (m); t is the time span for debris flowed from one point to the other (s).

In order to improve the precision, at each location, several different distinguished debris were selected to estimate the wave velocity repeatedly. The amount of debris used in each location is plotted in **Table 1**.

A velocity measurement of the debris at location B is described as an example. The time span for the debris flowed from one point to the other was obtained from the video. **Fig. 4** is drawn based on the video screen which shows the starting point for timing. When the debris passed Point A, from the timer of video, the time point was observed as 5sec. **Fig. 5** is drawn based on the video screen which shows the terminal point for timing. When the debris passed Point B, the time point was observed as 51sec. After that, the time span for the debris flowed from Point A to Point B was computed as 51-5 = 46sec.

Moreover the authors searched for the rough positions of Point A and B in the

Google Earth, with the use of Mark A and B, refer to **Fig. 6**. By the use of the distance measuring function of Google Earth, the distance between Point A and B was estimated around 290m. In the end, the Eq. (1) was applied to compute the velocity of the debris as 6.3m/s, refer to the velocity of B-2 in **Fig. 7**. By the same method, the wave velocity at location B was measured by 3 times with different debris. And the average velocity of the debris at location B was 6.4m/s. In the same way, the average wave velocities at the other 4 locations were computed as well. At last the average wave velocity of the 5 locations was computed as 5.1m/s, as shown in **Fig. 7**, and this velocity can be regarded as the average wave velocity in Tohoku Region.

Among the 16 velocity data, only the velocity of debris B-1 reached 7.0m/s, so it should be considered as an isolated phenomenon and the wave velocity at Utatsu Bridge should not exceed 7.0m/s. Besides that, since the Utatsu Bridge is located at location A (average: 5.9m/s) and the wave velocity is slightly larger than the velocity

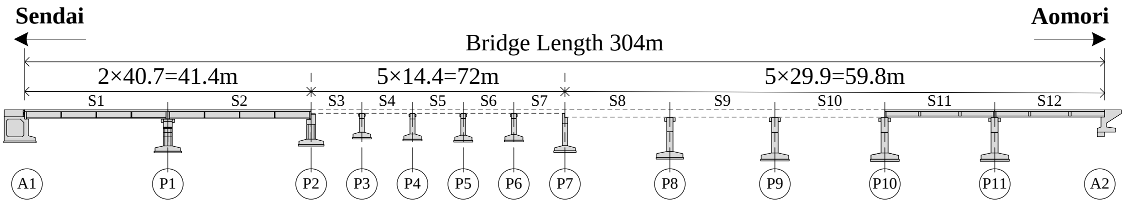

Fig. 8 Side view of Utatsu Bridge (before damaged, view from seaside)

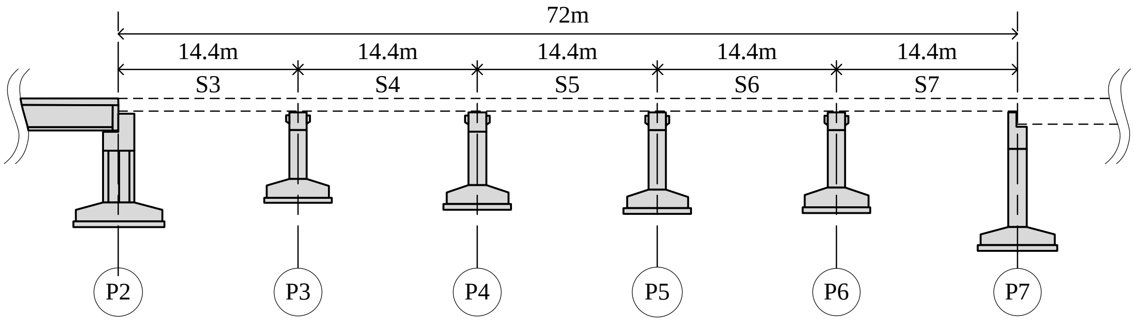

Fig. 9 Side view of damaged superstructures (S5~S7)

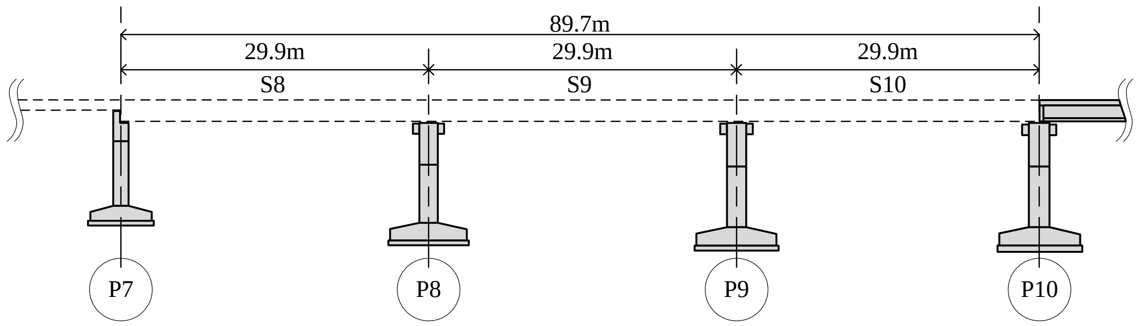

Fig. 10 Side view of superstructures (S8~S9)

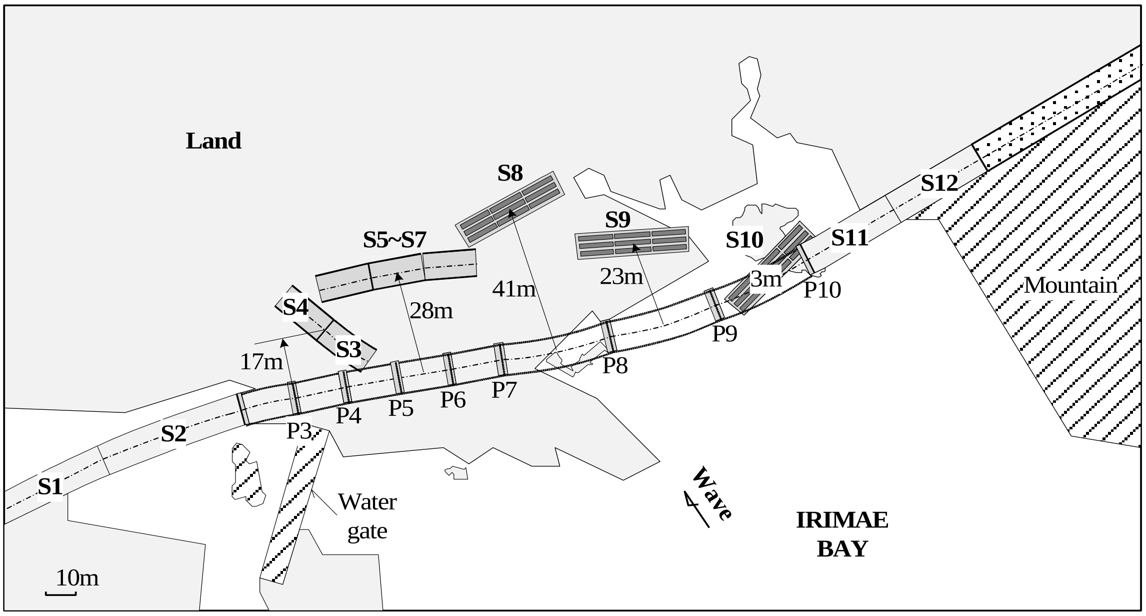

Fig. 11 Outflow condition of Utatsu Bridge

of debris due to the effect of obstacles, it is reasonable to define the wave velocity at Utatsu Bridge as 6.0m/s.

<u>Damage to Utatsu Bridge</u>

In the following content, the Utatsu Bridge which belongs to Line 45 of national road is analyzed as an example. The Utatsu Bridge, located at Minamisanriku Town over Irimae Bay, is composed of 3 types of superstructures varying in length from 14.4m to 40.7m, as shown in **Fig. 8**. For simplicity, the authors assigned numbers for the superstructures and piers from Sendai side to Aomori side. The 12 superstructures were numbered from S1 to S12 while the 11 piers were numbered from P1 to P11.

Based on the detailed survey, superstructures S3~S10 moved off their supports under the wave-induced lateral load while the superstructures of S1, S2, S11 and S12 did not flow out. In the flowed spans, S3~S7 and S8~S10 have different types and the details of them are shown in **Fig. 9** and **Fig. 10**. The displacements of S3~S10 have been illustrated in **Fig. 11**. The directions of displacements are transverse to the bridge axis. The characteristic of outflow condition is that the central spans such S5~S7 and S8 experienced long displacements (28m and 41m).

It was also observed that S3~S4 and S5~S7 flowed out with no separation. And due to a great wave-induced uplift force, S8~S10 were inverted when they flowed out.

However, contrary to the damage of superstructures, all piers of Utatsu Bridge withstand the wave action and did not collapse (**Fig. 12**, **Fig. 13)**. The main damage to the piers is that the concrete surfaces of beams dropped due to a collision with girders and most of bridge collapse preventions were crushed or flowed out.

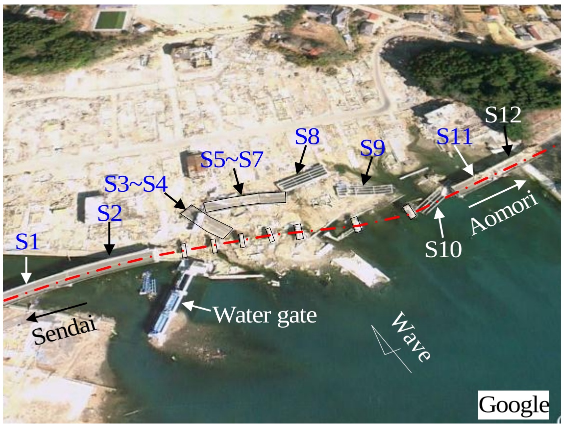

Fig. 12 Outflow condition

Fig. 13 General damage to piers

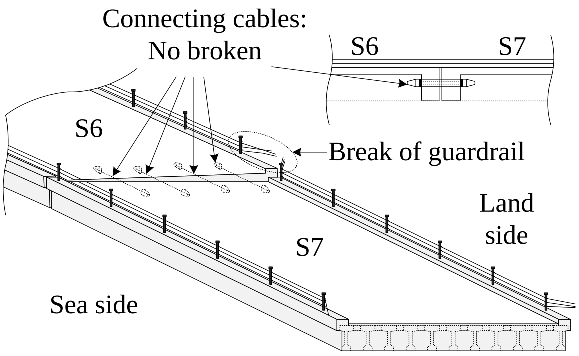

a. Damage to S6~S7

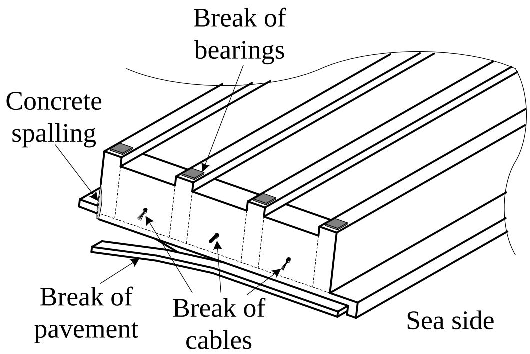

b. Damage to S9

Fig. 14 Detailed damage to superstructures

The damage to S3~S7 is one of the typical ones, which flowed out connecting with each other, and the damage of S6~S7 was selected as an example to state in the following content. Under the wave action, S6 and S7 experienced a displacement of 28m together thus it is proper to regard them as a whole. When the bridge was retrofitted, 4 cables, which were used to prevent the relative movement in axis direction of superstructures, were installed between S6 and S7. The details of cables are plotted in **Fig. 14-a**. These cables played an important role to keep S6 and S7 flowing out together. Besides, the damage to guardrails between S6 and S7was observed as well.

S9 is one of the inverted superstructures, the damage to which is shown in **Fig. 14-b**. S9 experienced a displacement of 23m and was inverted by the wave-induced uplift. At the end surface of S8 side, different from the damage to S6 and S7, all of the cables which connected S8 and S9 were broken by the force between superstructures and the fracture traces could be found. Moreover, at the supporting area of girders, the remains of bearing plates were noted. In light of this, it is obvious that during the tsunami attack the bearings fractured. Besides that, at the connection of the 2 decks, the debris of pavement connection was observed.

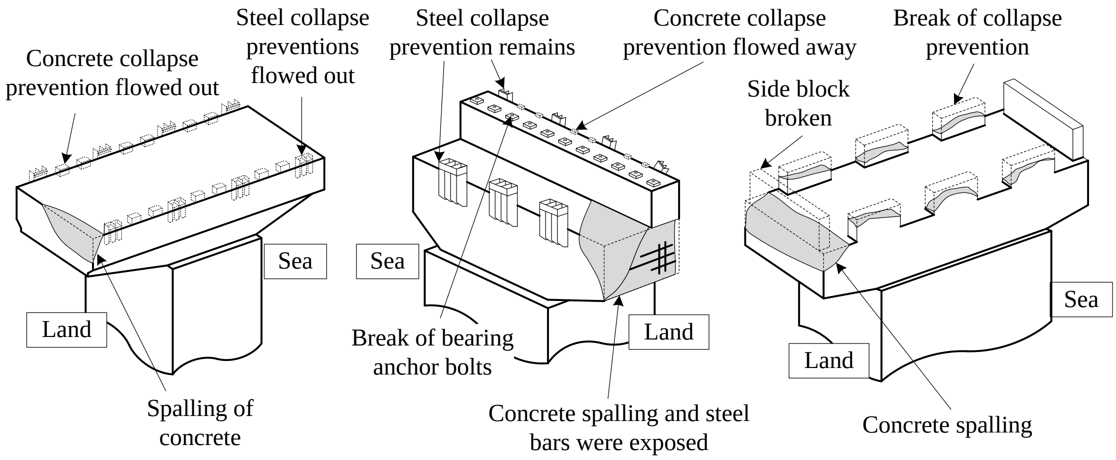

a. Damage to P6 **b. Damage to P7** **c. Damage to P8**

Fig. 15 Detailed damage to piers

It was found that the 11 piers supported 3 types of superstructures. In this section, 3 piers were selected basing on their different supporting superstructures. Pier 6 and Pier 8 respectively supported the type 2 and type 3 and in contrast, P7 supported both of these 2 types of superstructures (**Fig. 9**, **Fig. 10**). Therefore P6~P8 were selected to analyze. For P6 and P7, except for the concrete collapse preventions, they also had been installed steel preventions. Different from P6 and P7, only concrete collapse preventions were set up at the top of P8. These collapse preventions not only limit the superstructure's movement along the axis direction but also the transverse direction of bridge.

The detailed damage of P6 is shown in **Fig. 15-a**. When S6 and S7 were separated from P6, they imposed a horizontal collision on the concrete collapse preventions. Therefore, on the supporting plate of P6, 12 concrete collapse preventions were crushed. And for the same reason, the 8 steel collapse preventions, anchored on the sides of the beam, flowed out as well. Apart from the damage to the collapse preventions, the concrete surface of the beam which was located at the land side was crushed as well.

Fig. 15-b illustrates the detailed damage of P7 which supported 2 types of superstructures: S7 and S8. At S7 side, the installing details of superstructure collapse preventions were same as P6. Although the 6 concrete collapse preventions were crushed, the 4 steel ones were left. However, due to the girder-induced impact, the steel ones tilted. At S8 side, different from P6, only 3 larger steel collapse preventions were anchored and they did not flow out. The damage condition of steel collapse preventions demonstrates that when the superstructures, located on P7, displaced they were elevated by a wave-induced uplift. Because of this, the superstructures flowed from the top of the steel collapse preventions and did not impose a sufficient impact to make them separate from supports. Besides that, at the land side, the concrete surface of the beam was crushed and some steel bars could be observed.

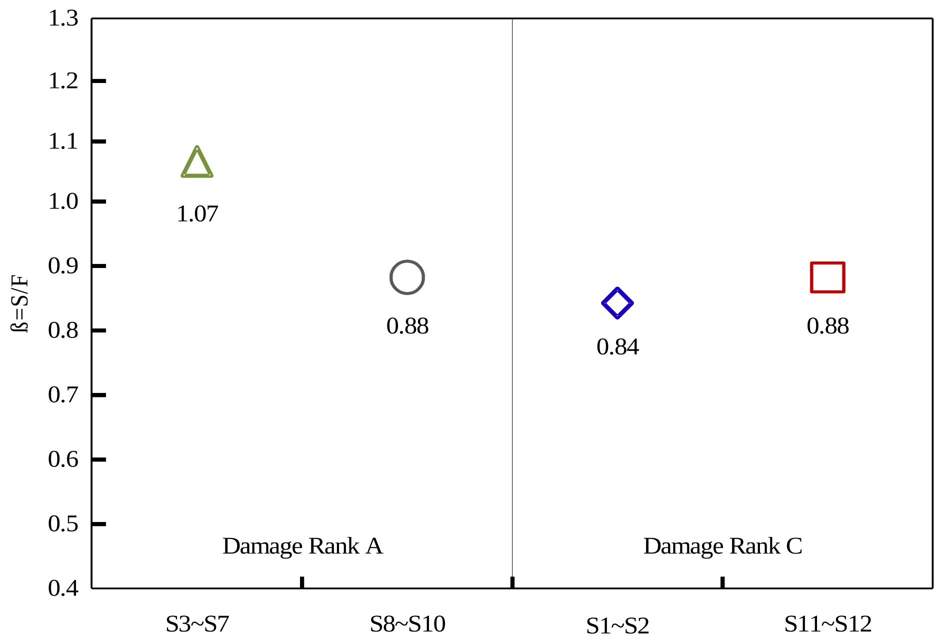

Fig. 16 β result of Utatsu Bridge

The damage of P8 is plotted in **Fig. 15-c**. On the top of beam, 6 concrete collapse preventions and 2 side concrete blocks were set up. By the same force situation as the preventions of P6, the 6 concrete collapse preventions and one side block, which was at the land side, were crushed. Besides, it was found while the side block flowed out, a damage of the concrete surface, which under the side block, occurred.

Simple Analysis of Utatsu Bridge

In this chapter, in order to confirm the outflow condition of Utatsu Bridge, the concept of ratio β to superstructure resistance and wave lateral load on is proposed. The relationship between the ratio and the outflow of girders has been analyzed. The expressions to compute the ratio β are listed as follows (Kosa, 2010):

$$\beta = \frac{S}{F} \tag{2}$$

$$S = \mu W \tag{3}$$

$$F = \frac{1}{2}\rho_w C_d v^2 A \tag{4}$$

Where, β is the ratio to resistance and lateral load; F is wave lateral load (kN); S is superstructure resistance (kN).

When computing β values, based on the result of last chapter, it is reasonable to apply v=6.0m/s. Further, based on the former experimental result the friction coefficient will be assumed as 0.6. For comparison, the damage extents of bridge

Table 2 Details of damaged bridges in Tohoku Region

Object Bridge	Object of Span(s)	Girder Type	Damage Rank	Span Length	Bridge Width	Bridge Height	Ratio β
				L[m]	B[m]	D[m]	
Utatsu Bridge	9th Span	Simple Post-Tension "T" Girder	A	29.9	8.3	2.5	0.89
Koizumi Bride	1st-6th Span	Continurous Steel Plate Girder	A	181.8	11.3	2.6	0.90
Kesen Bridge	1st-5th Span	Continurous Steel Plate Girder	A	181.1	13.3	2.7	0.99
Kawaharagawa Bridge	1st Span	Simple PC Hollow Girder	C	28.8	14.8	1.8	4.30
Nijyuichihama Bridge	1st Span	Simple Pre-Tension "T" Girder	C	16.6	8.3	1.5	1.23
Hamadagawa Bridge	1st Span	Simple Post-Tension "T" Girder	C	22.5	14.8	1.7	2.64
Numata-Kosen Bridge	2nd Span	Simple Post-Tension "T" Girder	A	20.0	13.5	2.6	1.34
Namiita Bridge	1st Span	Simple Pre-Tension "T" Girder	C	12.5	9.2	1.3	0.88
Sodeogawa Bridge	1st-4th Span	Continurous RC hollow Girder	C	59.9	8.8	1.5	1.83
Mizujiri Bridge	3rd Span	Simple Steel "H" Girder	A	10.5	5.9	1.4	0.61
Shinkitagami Bridge	1st, 2nd Span	Continurous Steel Truss Girder	A	155.0	8.6	3.6	0.45
Shiomi Bridge	1st Span	Simple PC "I" Girder	C	13.5	11.3	1.365	4.31
Shin-Aikawa Bridge	1st Span	Simple Steel Box Girder	A	67.2	11	3.835	0.57
Hachiman Railway Bridge	1st Span	Simple Post-Tension "I" Girder	A	22.9	5.5	2.05	0.62
Hachiman Highway Bridge	1st-3rd Span	Simple Post-Tension "I" Girder	C	12	8.2	1.07	5.97

girders is described by Rank A, B and C. Rank A means girders separated with substructures completely. Rank B means girders suffered displacements but still can be used. Rank C means girders only suffered partial damage such as damage to guardrails.

The β result is illustrated in **Fig. 16**. Based on **Fig. 16,** it is known that S3~S10 suffered damage Rank A and the remaining girders suffered damage Rank C. Most β values are smaller than 1.0 except for the β values of S3~S7 which is 1.07, slightly larger than 1.0. This trend of β values illustrates, comparing with wave lateral load, superstructure resistance is not sufficient to make S3~S10 survive, which is attributed to the relatively small girder width causing the comparatively small girder weight.

Simple Analysis of Bridges Damaged Due to Tsunami

Except for the Utatsu Bridge, 12 other damaged bridges in Tohoku region, the details of which are shown in **Table 2**, and the damaged bridges due to the Sumatra Earthquake have been analyzed as well. By the same method in last chapter, the β values of them are obtained and illustrated in **Fig. 17**.

Fig. 17-a and **Fig. 17-b** illustrate the β values of damaged bridges in Tohoku

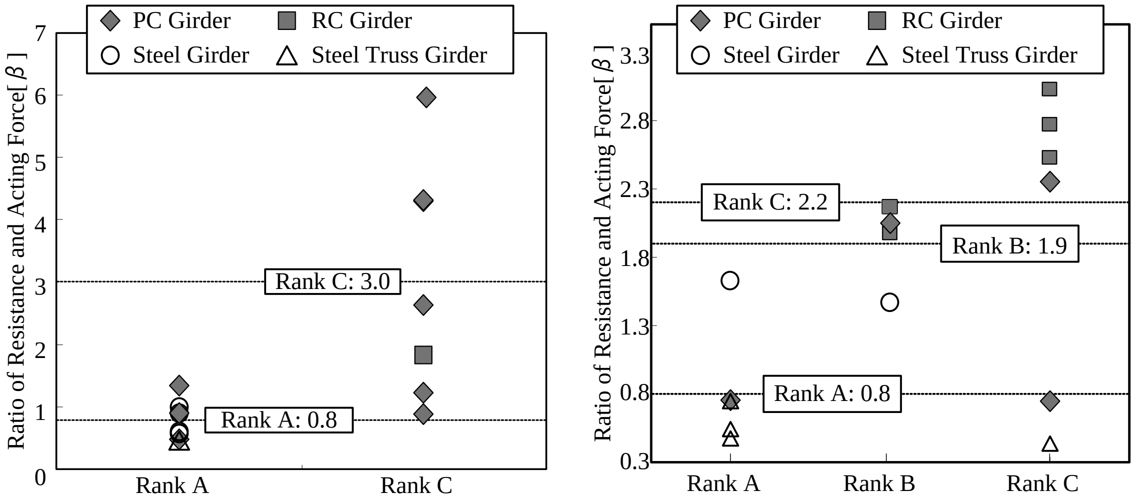

a. Great East Japan Earthquake **b. Sumatra Earthquake**

Fig. 17 β result of Sumatra and Great East Japan Earthquake

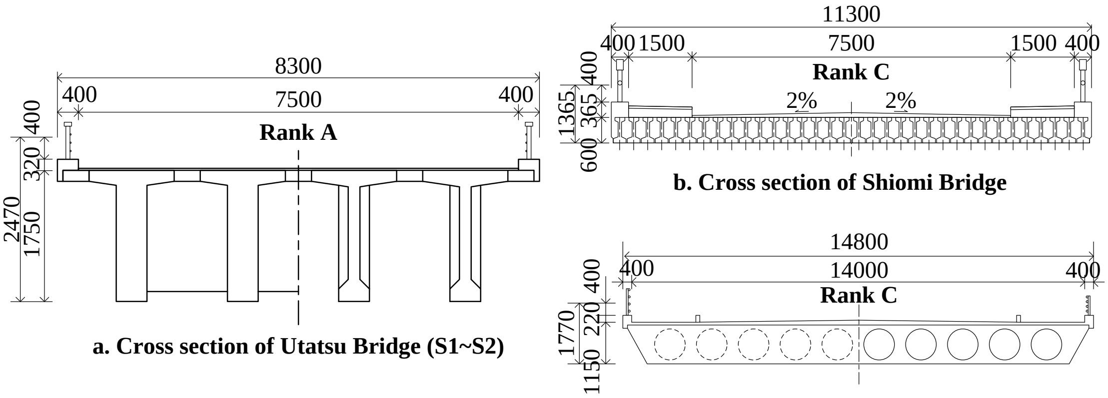

a. Cross section of Utatsu Bridge (S1~S2)

b. Cross section of Shiomi Bridge

c. Cross section of Kawaharagawa Bridge

Fig. 18 Comparison of cross sections

region and the bridges damaged in Sumatra Earthquake respectively. In terms of the relationship between damage extents and β values, according to the former research as shown in **Fig. 17-a**, during the Sumatra Earthquake, the average β values of Rank A, Rank B and Rank C are respectively 0.8, 1.9 and 2.2 and the average β value of Rank A is around 2.5 times larger than Rank C. By the same method, for the situation of bridges in Tohoku region, refer to **Fig. 17-b**, the average β values of Rank A and Rank C are 0.8 and 3.0 respectively. And the average β value of Rank A is around 3.75 times larger than Rank C. Therefore, from the above result, it is noted that the β value is a significant indicator to judge the damage extent of bridges.

Fig. 18 is applied to describe the difference of typical girders of Rank A and Rank C. It is obvious that the ratio to girder width and height of Rank A (3.36) is smaller comparing with the girder of Rank C (b: 8.28, c: 8.36), which led to insufficient resistance and greater wave pressure area. Therefore, in future design, it should be considered to increase the ratio to girder width and height for tsunami resistance.

Conclusions

(1) Among the undated 3000 bridges subjected to the earthquake, around 10% suffered serious damage and could not be used.

(2) Based on the flow velocities of debris in 5 inshore locations during the tsunami attack, the wave velocity at Utatsu Bridge can be estimated as 6.0m/s.

(3) Based on the field survey, for the damage to the superstructures of Utatsu Bridge, S3~S10 experienced movement and for the damage to piers, although they did not collapse, the devices, which were used to prevent the collapse of superstructures, such as RC blocks, steel brackets and anchor bolts suffered serious loss.

(4) With the comparison of damage appearances of bridges in Sumatra Earthquake and the bridges in Tohoku Region. As a result, when the tsunami heights were excess of 10m, the damage to bridges in 2 sites have many common points: outflow of girders and scour of foundations.

(5) With the comparison of the β ratios of the damaged bridges in Sumatra Earthquake and the bridges in Tohoku Region. As a consequence, the β ratios of the bridges with same damage rank have the similar degrees, especially for the bridges of Rank A. Therefore, in the future work, it is reasonable to apply β ratio as the indicator to justify the function against tsunami of bridges.

References

1. Japan Meteorological Agency (JMA): The 2011 Off the Pacific Coast of Tohoku Earthquake (Quick Report #25), Strong 105 Reference Material 4 by the Subcommittee for Evaluation of Strong Ground Motion, the Earthquake Research Committee, 2011.

2. Li, Damage Analysis of Utatsu Bridge Affected by Tsunami due to Great East Japan Earthquake, The 14th Symposium on seismic design of bridges, The Earthquake Engineering Committee, Journal of Structural Engineering, pp .111-118, 2011. 7.

3. Kosa, Analysis of Damaged Bridge by Tsunami due to Sumatra Earthquake, Journal of Structural Engineering, Vol.55A, pp .483-494, 2010. 3.